Location and Diffusion of respiratory gases (O$_2$ and CO$_2$) in nano-segregated fluids

João Filipe Viana de Sousa [†][*]

Supervisors: Prof. Doctor Eduardo Jorge Morilla Filipe[†]and Prof. Doctor George Jackson[‡]

Abstract

The respiratory gases, oxygen and carbon dioxide in particular, are often said to be fluorophilic as they seem to display enhanced solubilities in perfluorinated solvents. However, this behavior is far from being fully understood, or even confirmed. In this work the subject was addressed using molecular simulations. Solutions of O$_2$ and CO$_2$ in hexane and perfluorohexane at infinite dilution were simulated. The atomistic OPLS-AA force field was used and both molecular dynamics and the Widom particle insertion methods were performed. From the simulation results structural, energetic and transport properties were obtained: solute-solvent interaction energies; solvation enthalpies; Henry's constants; diffusion coefficients; preferential location of the solutes in the pure solvent's structure. Mixtures of hydrogenated and perfluorinated liquids have been shown to nano-segregate forming distinct hydrogenated and perfluorinated domains. This has been previously demonstrated experimentally using xenon NMR spectroscopy and confirmed by MD simulations. Those results clearly show that the xenon particle is able to detect the existence of such domains, dissolving preferentially in hydrogenated environment. Following the same strategy, in this work infinite dilution solutions of oxygen and carbon dioxide in mixtures of hexane + perfluorohexane and hexanol + perfluorohexanol were also simulated. From the simulation results no particular interaction or preferential location of O$_2$ and CO$_2$ towards perfluorinated solvents could be identified. Thus, any enhanced solubility of the gases in these solvents is probably due to the existence of cavities intrinsic to the liquid structure of the perfluorinated solvents.

Keywords: Molecular Dynamics Simulations, Fluorinated Compounds, Respiratory Gases

Introduction

Perfluoroalkanes are organic molecules composed of a saturated carbon chain bonded with fluorine atoms, like regular alkanes but with fluorine instead of hydrogen. This substitution translates to a larger cross-sectional area for the fluorinated chains resulting in higher densities and molar volumes when comparing with their n-alkanes counterparts [1]. When compared to their alkane counterparts, perfluoroalkanes display higher vapour pressures and lower surface tensions due to the low polarizability of the fluorine atom and the weak dispersion forces it creates in the perfluorinated compounds, making them non-flammable compounds with useful applications as fire retardants [2] [3]. Furthermore, there are conformational differences noted between the two chains: the n-alkanes display an all-trans planar form due to their dihedral angle at the energy minimum, while the fluorinated chains present a helical conformation making them rigid in comparison to the hydrogenated chains which have a flexible character. Some authors suggest that the stiffness displayed by the fluorinated chains, due to its less efficient molecular packing, is responsible for the formation of empty spaces between molecules in liquid fluorocarbons, which can explain the higher solubility in respiratory gases shown by perfluoroalkanes [3].

Mixtures of hydrogenated and perfluorinated compounds, in particular, mixtures of alkanes and perfluoroalkanes, despite the very similar intermolecular forces, are known to be highly nonideal displaying large positive deviations to Raoult's law, very large positive excess volumes, and very large positive excess Gibbs energy and enthalpy [2]. They also display liquid-liquid immiscibility ranges. Perfluoroalkanes and alkanes are mutually phobic. Furthermore, several works demonstrated that perfluoroalkane/alkane mixtures exhibit nano-segregated domains [4] [5]. Mixtures of alkanes and perfluoroalkanes have been extensively studied in past years, however the reason for this mutual phobicity is still poorly understood.

More recently the focus has shifted to the much less documented mixtures of fluorinated and hydrogenated alcohols. In mixtures of perfluorinated+hydrogenated alcohols, the structure of the liquid results from the balance between preferential hydrogen bonding between the hydroxyl groups of the hydrogenated and fluorinated alcohols and the unfavourable dispersion forces between the hydrogenated and fluorinated chains. With the increase in chain length, the contribution of dispersion increases and eventually overcomes the contribution of the H-bonds, contributing to the segregation between hydrogenated and fluorinated segments [5]. Like perfluoroalkane+alkane mixtures, the mixtures of alcohols display large positive excess molar volumes but, on the other hand, the excess molar Gibbs energy ranges from large and negative to large and positive [5] [6].

The interest in studying these fluorinated compounds and their distinctive chemical and mechanical behaviour comes from their wide range of important applications in various fields like medicine or the industry with new applications being discovered every year. In terms of industrial applications, they are used in the production of lubricants, propellants, surfactants, surface coating films (like water and stain repellents), anticorrosives and as cleaning and drying solvents [7] [8]. Moreover, they can also be used in fire extinguishing foams [7] [9]. Although they serve many purposes their main application still is as refrigerants as it is an essential feature in industry and in day-to-day life [7]. For medical purposes, the fluorinated compounds have very important applications as drug delivery agents [10], they also facilitate the transport of oxygen [11] and are used in many anaesthetics [7].

The solubility of respiratory gases in hydrogenated and fluorinated compounds is a prevailing important topic, in particular in the context of carbon capture. CO$_2$ and O$_2$ are often said to be more soluble in perfluorinated solvents than their hydrogenated counterparts. However, the subject is far from being fully understood or even proved.

Part of the effect is sometimes justified by the less compact liquid organization of perfluoroalkanes which generates voids in the liquid that small gas molecules can fill [12] [13]. Several studies have been made with the aim of comparing the affinity and interaction of carbon dioxide with fluorocarbons and hydrocarbons. CO$_2$ is normally modelled placing positive partial charges on the carbon atom and negative partial charges on the oxygen atoms. The molecule can thus behave as a weak Lewis base and as a weak Lewis acid in terms of intermolecular interactions. Raveen-

[*]E-mail: joao.viana.sousa@tecnico.ulisboa.pt
[†]Instituto Superior Técnico, Universidade de Lisboa, Lisboa, Portugal
[‡]Imperial College, London, United Kingdom

dran reported that the CO_2 molecule interacts with fluorocarbons through the carbon atom while the interactions with hydrocarbons occur through the oxygen atoms [14]. These studies raised more questions about the preferential affinity of CO_2 molecules for fluorinated or hydrogenated compounds and the results have been conflicting depending on the studied substances. Computational studies by Cece [15] reported positive interaction energies between carbon dioxide and fluorinated molecules and very small interaction energies with hydrogenated molecules. Furthermore, NMR measures made by Dardin [16] also show specific attractive interactions between CO_2 and fluorinated compounds corroborating the previous studies done by Cece. However, infrared [17] and further NMR [18] experiments did not show evidence of a particular interaction between CO_2 and fluorocarbons. Yee [17] reported that the enhanced solubility of fluorocarbons in supercritical CO_2 was due to the highly repulsive fluorocarbon-fluorocarbon interactions favouring solute-solvent interactions. It was also reported by Padua [19], in a computational approach, that there was no evidence of a particular affinity between fluorocarbons and CO_2. In a recent preliminary study by Monteiro [20] the affinity of CO_2 for hydrogenated and fluorinated alcohols was evaluated at infinite dilution by molecular dynamics simulations, finding no evidence of CO_2 preference for the fluorinated solvents. In conclusion, further investigations on the topic are needed, as well as for other interesting and important respiratory gases such as oxygen and nitrogen.

Simulation Procedure

MD simulation details Molecular dynamics simulations were performed to get a better understanding of the behaviour of CO_2 and O_2 molecules at infinite dilution in systems of fluorinated and hydrogenated solvents. For this study two alkanes were used, Perfluorohexane (PFH) and Hexane (Hex), as well as two alcohols, Perfluorohexanol (UFH) and Hexanol (HexOH).

To run all the molecular dynamics simulations an open-source package of GROMACS (Version 2018) [21] was used. The systems of molecules were fit in cubic boxes with periodic boundary conditions for all directions and a time step of 2 fs. The simulations were performed in boxes containing 300 molecules of solvent and 1 molecule of either CO_2, O_2 or Xe, maintaining the system size and changing the ratio of fluorinated to hydrogenated solvent. The systems that analysed the behaviour of the pure solvents to facilitate the determination of the solvation energy were composed of only 300 solvent molecules.

To carry out the molecular simulations the following procedure was performed:

1st – A box was generated containing the necessary molecules all randomly placed. The box was then submitted to an energy minimization phase for 20000 steps without temperature or pressure control, bringing the system to a lower energy state.

2nd – The resulting box from the first step was then submitted to an equilibration phase in NPT (meaning the number of particles, pressure and temperature are specified) ensemble for 1 ns and 500000 steps at a temperature of 600K and a pressure of 200 atm. During this stage the temperature and pressure were controlled with the Beredensen thermostat and barostat.

3rd – The box was then submitted to the production step in NPT ensemble for 30 ns, to get good statistics of the behaviour of the probe molecules in the mixtures, or 100 ns only for the simulations where potential energy values with low uncertainty were needed. This step was done at 1 atm and at three different temperatures, 283.15 K, 298.15 K and 313.15 K to study the influence of temperature in some properties. During this stage the pressure was controlled with the Parrinello-Rahman barostat [22], and the temperature was controlled with the Nosé-Hoover thermostat [23].

The force field models used were OPLS-AA, the atomistic optimized potential for liquid simulations all-atom [24] [25] and the L-OPLS-AA [26] which is an extension of the former force field but for longer hydrocarbon chains. The parameters used for Hexanol and Hexane molecules are published on papers [27] [26]. For the fluorinated chains more parameters were needed to complete the force field and simulate their behaviour realistically. To describe the CF_3-CF_2 interactions the parameters were taken from the OPLS-AA work on perfluoroalkanes [25], for the CF_3-CF_2-OH interactions the force field parameters were developed by Duffy [28]. The remaining dihedral torsion parameters were obtained from work [29] by Padua. The parameters of the CO_2 molecule were obtained from a paper by Harris and Yung [30], for the O_2 molecule the parameters were taken from a paper by Miyano [31] and for Xe the paper by Fischer and Kohler [32] was used.

The non-bonded Lennard-Jones interactions between different types of sites are calculated by geometrical mean rules for both energy and size, equations 1 and 2 respectively.

$$\varepsilon_{ij} = \sqrt{\varepsilon_{ii} \cdot \varepsilon_{jj}} \qquad (1)$$

$$\sigma_{ij} = \sqrt{\sigma_{ii} \cdot \sigma_{jj}} \qquad (2)$$

These energy and diameter cross-interactions are not properly designed for the weak unlike interactions between the hydrogenated and fluorinated chains in the mixtures [33] to replicate experimental excess properties. Some corrections were made by adding a corrective factor to each of these parameters. For the energy cross-interaction a factor of $\xi = 0.77$ was implemented and for the size cross-interaction the factor was $\eta = 1.035$, these were suggested by Morgado et al. for the L-OPLS-AA force field [5] [34].

For the same molecule, only atoms separated by three or more bonds are considered for the non-bonded interactions between atoms. Both Lennard-Jones and the long-range electrostatic (Coulomb) interactions were truncated by using cut-offs of 14 Å. To calculate the long-range Coulomb interactions, beyond the cut-off, the Particle-Mesh Ewald (PME) method was used. All bonds involving Hydrogen atoms were considered as rigid by being restricted to their equilibrium lengths, using the LINCS algorithm [35]. For all simulations, a neighbour list with a radius of 10 Å was used and updated every 10 steps.

To determine the Henry's constant and solubility of Xe, CO_2 and O_2 in the solvents the test-particle insertion (TPI) method was used [36]. To use this method a simulation box with only the pure solvent was created according to the three previously described steps. The box, using the TPI logarithm, is then submitted to multiple random insertions of the solute molecule, in this case 1000 insertions per frame with a radius of insertion of 0.02 nm.

Property Studies The densities of the mixtures were obtained directly from the average volume of the box. The excess molar volume of the mixtures was calculated through equation 3 where x is the molar fraction, M represents the molar mass and ρ is the density.

$$V_M^E = \frac{x_1 M_1 + x_2 M_2}{\rho} - \frac{x_1 M_1}{\rho_1} - \frac{x_2 M_2}{\rho_2} \qquad (3)$$

The Henry's constant was calculated through equation 4 where μ_2 is the chemical potential of the solute, determined by GROMACS using the TPI method, ρ_1 is the density of the solvent, R is the ideal gas constant and T is the temperature of the solution.

$$H_{2,1} = \lim_{x_2 \to 0} \left[RT\rho_1 \cdot exp\left(\frac{\mu_2^r}{RT}\right) \right] \qquad (4)$$

The solvation enthalpies of Xe, CO_2 and O_2 were calculated through the difference between the potential energy of the solution, for each solute, and the potential energy of the solvent. The potential energy was obtained directly from GROMACS.

To analyse the solvent structure and to check the preferred location of the CO_2 and O_2 molecules in the mixtures, the method chosen was to compute the radial distribution functions (RDFs) which determine the density of probability of finding a particle at a distance r from a reference particle, equation 5.

$$g(r) = \frac{1}{N\rho} \sum_{i}^{N} \sum_{j \neq i} \delta(r - r_{ij}) \tag{5}$$

First, the RDFs were performed between the fluorinated and hydrogenated solvents to study the solvent structure of the mixtures, then they were performed between the solute molecules and the solvents to identify the preferred location of CO_2 and O_2 molecules.

Using the RDFs, another parameter that was determined was the local composition around the solute molecules. It was necessary to determine the number of fluorine and hydrogen neighbours for each solute molecule through the RDFs and cumulatives of the interactions solute-F and solute-H . The distance considered to calculate the number of neighbours was the relative minimum of the solute-F RDF, since fluorine is bigger than hydrogen. With the number of neighbours taken from the RDF's cumulatives it was possible to calculate the local composition of the mixtures from the ratio between the number of fluorine neighbours and the total number of neighbours.

The diffusion coefficients for Hex, HexOH, PFH, UFH, CO_2 and O_2 in the mixtures studied at different compositions were calculated using the Einstein equation 6.

$$D_0 = \frac{1}{6N} \lim_{t \to \infty} \frac{d}{dt} \sum_{N}^{i=1} \left\langle |r_i(t) - r_i(0)|^2 \right\rangle \tag{6}$$

In equation 6, $|r_i(t) - r_i(0)|^2$ is the mean squared displacement of a single solute molecule averaged over time. To calculate the diffusion coefficient through the simulations, first the mean squared displacement was computed for intervals of 5 ns for all 30 ns of the simulations. Then the slope of the linear part of the MSD function was determined for each interval. The mean value of the slopes was then calculated resulting in the diffusion coefficient. Since the Einstein equation doesn't consider the the size of the simulation box, a corrective factor [37] was applied in equation 7 resulting in the corrected diffusion coefficient. Where k_B is the Boltzmann constant [38], T is the temperature of the simulations, ξ is an empirical factor of 2.837297 [37], L is the length of the box and η is the viscosity of the solvent.

$$D = D_0 + \frac{k_B T \xi}{6\pi\eta L} \tag{7}$$

The viscosities used for the PFH+Hex mixture were the experimental data obtained by Morgado shown in paper [1] and for the mixture of UFH+HexOH the experimental viscosities were taken from work [39] by Miguel Costa.

The hydrodynamic radius, R, was then calculated through the equation of Stokes-Einstein 8, using the diffusivities previously determined and the experimental viscosities taken from the literature already cited.

$$D = \frac{k_B T}{C\pi\eta R} \tag{8}$$

The interaction energies between the respiratory gases and the solvents were calculated by the sum of the Coulomb and Lennard-Jones interaction energies, which were obtained directly from GROMACS.

Results and Discussion

Mixtures of Hydrogenated and Fluorinated Solvents

Excess Molar Volumes: Force Field Validation The excess molar volumes of the mixtures (Hex+PFH) and (HexOH+UFH) were calculated at 298.15K and atmospheric pressure, to assess if the simulations are a good representation of reality. The solvent mixtures should have been simulated without any solute particles (CO_2 or O_2). However it was considered that the presence of a single molecule of CO_2 or O_2 would not affect significantly the properties of the solvent mixtures. Therefore, the following results for the solvent properties were obtained from simulations that include a molecule of solute. The excess molar volumes are plotted in figure 1 for Hex+PFH mixtures where they are compared with experimental values [40]. For HexOH+UFH mixtures the excess molar volumes are presented in figure 2 and are also compared to experimental data [41].
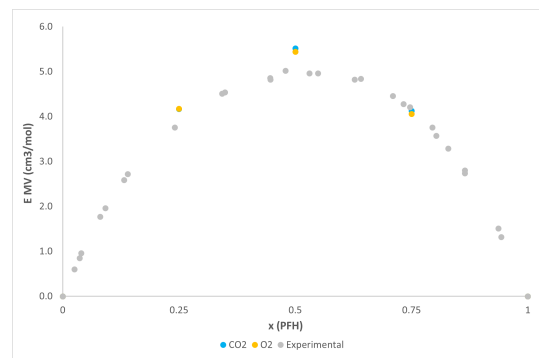

Figure 1: Excess molar volumes of Hex+PFH mixtures at 298.15 K and atmospheric pressure. Blue - simulations with CO_2; Yellow - simulations with O_2; Grey - experimental data.
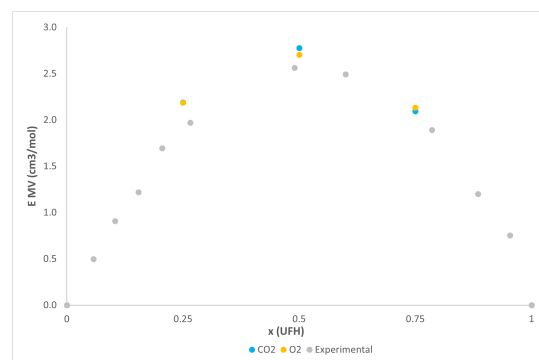

Figure 2: Excess molar volumes of HexOH+UFH mixtures at 298.15 K and atmospheric pressure. Blue - simulations with one CO_2 molecule; Yellow - simulations with one O_2 molecule; Grey - experimental data.

As can be seen, the excess molar volumes obtained from MD simulations agree with the experimental data. As previously mentioned, it has been shown in previous studies that the unlike interactions between the hydrogenated and fluorinated chains must be corrected relatively to the geometric mean rule. With these corrections $\xi = 0.77$ and $\eta = 1.035$ [4] the simulations reproduce well the experimental excess molar volumes of the mixtures. It is important to understand that the prediction of excess molar volumes is a difficult test to any computational method so by obtaining matching results with experimental data

it assures us that these models are very good at representing the interactions within the systems.

Liquid Structure of (Hydrogenated+Fluorinated) Mixtures To study the liquid structure of the PFH+Hex and UFH+HexOH systems the radial distribution functions (RDFs) were computed. The RDFs generated for the Hex+PFH and HexOH+UFH are displayed in figures 3 and 4, respectively.
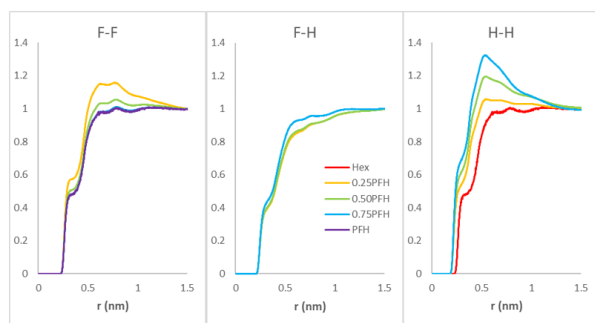

Figure 3: Intermolecular RDFs between hydrogen and fluorine atoms at 298.15K for mixtures of Hexane and PFH at different compositions; Red - Hexane; Yellow - 0.25 PFH; Green - 0.5 PFH; Blue - 0.75 PFH; Purple - PFH.
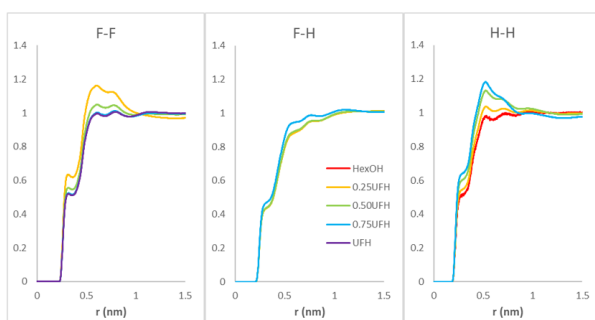
Figure 4: Intermolecular RDFs between hydrogen and fluorine atoms at 298.15K for mixtures of Hexanol and UFH at different compositions; Red - Hexanol; Yellow - 0.25 UFH; Green - 0.5 UFH; Blue - 0.75 UFH; Purple - UFH.

As can be seen, the RDFs between hydrogenated and fluorinated chains have low intensity for all mixtures, which means there is a lower probability of them being neighbours, leaning towards nano-segregation of the hydrogenated and fluorinated molecules and formation of domains. The intensity of the F-F peaks increases with the increase in hydrogenated compound concentration. The reverse happens to the intensity of the H-H peaks, it increases with the fluorinated compound concentration. This was verified for alkanes and alcohols alike. This is an indication that fluorinated chains are mainly surrounded by fluorinated chains and that hydrogenated chains are mainly surrounded by hydrogenated chains. These results seem to prove the existence of fluorinated and hydrogenated domains, as can be seen in figure 5 that shows a snapshot of the simulations ran for the equimolar mixtures. Finally, it's also worth to compare both alkane and alcohol mixtures. The alkane RDF peaks of H-H and F-F interactions are more intense than the same peaks of the alcohol mixtures, and the peaks of F-H interactions are lower in the alkane mixtures, indicating that there is a higher degree of nano-segregation in the alkane mixtures. The results from work [4] by Morgado et al., where xenon NMR spectroscopy and MD simulations were used, support the results from this study.
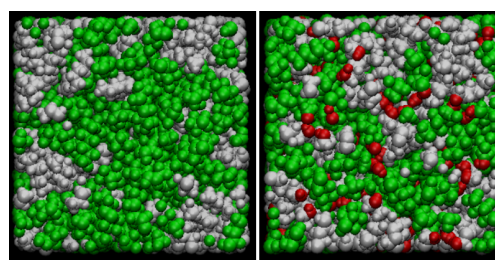

Figure 5: Snapshot of MD simulation boxes of two equimolar mixtures, Hex+PFH on the left and HexOH+UFH on the right; Green - PFH and UFH; White - Hexane and Hexanol; Red - Hydroxyl group.

Solutions of Xe, CO_2 and O_2: Parametrization of Solute-Solvent Cross Interactions

Solubility and Henry's Constant As previously mentioned the TPI method was used to calculate the Henry's constants of Xe, CO_2 and O_2, at atmospheric pressure and three different temperatures (10ºC, 25ºC and 40ºC), to study their solubilities in Hexane and Perfluorohexane. Xenon was included in the study as a comparison particle as it has been extensively studied in our research group. The results are shown in figures 6, 7 and 8. For Xe the results are compared to experimental data obtained by Pollack et al. [42] [43] and to previous simulations done by Pádua et al. [44]. For CO_2 the TPI method results are compared to previous simulations done by Pádua et al. [19]. The O_2 simulation results are compared to experimental data obtained by Pádua et al. [45].
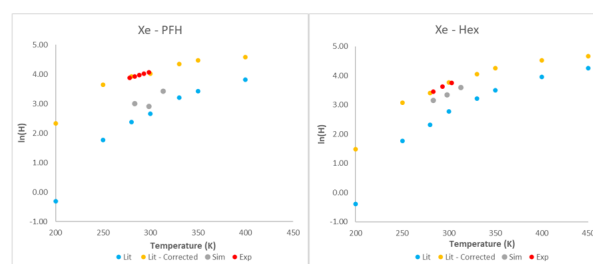

Figure 6: Henry's Constant for Xe in perfluorohexane (left) and hexane (right) at different temperatures and atmospheric pressure. Blue - simulations by Pádua et al.; Yellow - simulations with adjusted energy interaction parameter by Pádua et al.; Grey - simulation results; Red - experimental data by Pollack et al.
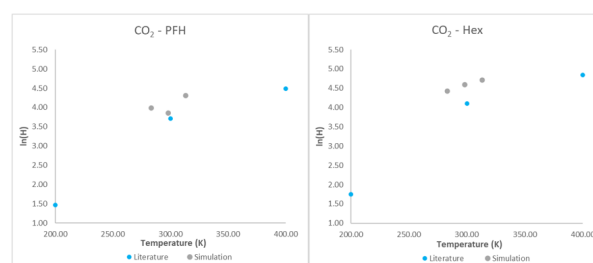

Figure 7: Henry's Constant for CO_2 in perfluorohexane (left) and hexane (right) at different temperatures and atmospheric pressure. Blue - simulations by Pádua et al.; Grey - simulation results.

As can be seen, from figure 6 the experimental solubilities of Xenon are higher in hexane than in perfluorohexane, as the Henry's constant is inversely proportional to solubility. The simulated results of Xe in hexane seem to replicate well enough the experimental results. However the simulated solutions of Xe in PFH present a positive deviation of solubility when compared to
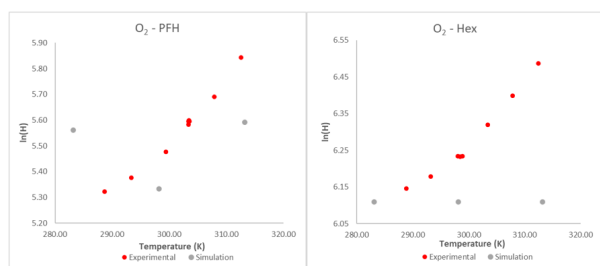
Figure 8: Henry's Constant for O_2 in perfluorohexane (left) and hexane (right) at different temperatures and atmospheric pressure. Red - experimental data by Pádua et al.; Grey - simulation results.

the experimental results. This can be an indication that the energy cross interaction parameter between xenon and PFH needs to be slightly decreased. Pádua used a correction to the unlike energy parameter between xenon and PFH $\xi=0.820$, so a similar correction should be used in our case. From figure 7 it's possible to see that CO_2 is more soluble in PFH than in hexane. The solubilities calculated for CO_2 are close to those obtained by Pádua et al. [19]. There is no experimental data for this mixture but it's possible to compare the ratio of solubilities PFH/Hex to the experimental ratio of perfluoroheptane/heptane [19]. For the mixture of PFH+Hex the determined ratio is around 1.71 and for the mixture of perfluoroheptane+heptane it's around 1.73 [19]. As there is no evident reason for the ratios to be different, since the molecules in question are very similar in size and properties, it is an indication that similar adjustments would be needed for the cross interactions between CO_2 and the two solvents. Since there is no experimental data for the solubility of CO_2 in each solvent, it is not possible to conclude if corrections for the cross interaction are needed. As for O_2, it can be seen from figure 8 that the simulated solubilities show a positive deviation when compared to the experimental data, with the exception of the solubility of oxygen in PFH at 10ºC which shows a negative deviation. Although the simulated solubilities of O_2 reproduce quite well the experimental data, a slight adjustment to the energy cross interactions between O_2 and the solvents might be needed. However, this conclusion is difficult considering the uncertainty of the simulation results. Performing more simulations at more temperatures would be advisable. When comparing the solubilities of the three solutes it's possible to see that Xe has the highest solubility followed by carbon dioxide, oxygen has the lowest solubility.

Solvation Enthalpy The solvation enthalpies of Xe, CO_2 and O_2 in hexane and PFH were calculated at atmospheric pressure and at different temperatures, the results are displayed in figure 9. For CO_2 no experimental data was found to compare the simulation results.
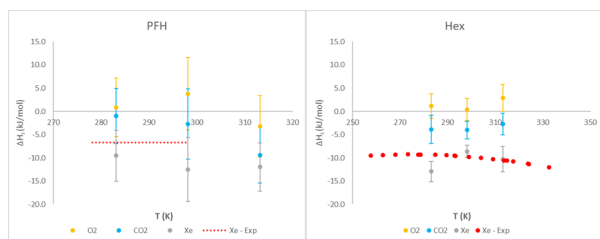

Figure 9: Simulated solvation enthalpy of Xe (Grey), CO_2 (Yellow) and O_2 (Blue) at different temperatures and atmospheric pressure, in perfluorohexane (left) and hexane (right). Experimental $\Delta \bar{H}_s$ of Xe in PFH (Red dotted line) and experimental ΔH_s of Xe in hexane (Red).

As can be seen from figure 9, for both solvents, Xe has the largest (more negative) solvation enthalpy followed by CO_2 and

then O_2. The simulated solvation enthalpies of Xe in hexane reproduce well the experimental results obtained by Martins et al. [46], which is a good indication that the simulations performed are a good representation of the real behaviour of the solutions and the energy interaction parameter between Xe and Hex does not need to be adjusted. For Xe in PFH, Pollack et al. [43] determined the mean solvation enthalpy, $\Delta \bar{H}_s$, between 5ºC and 25ºC, represented by the dotted red line in figure 9, which fits within the standard deviation of our simulation results indicating that a slight adjustment of the parameters might be needed. According to Pádua et al. [45], the experimental solvation enthalpies of O_2 vary between 0 and -26 kJ/mol in a short range of temperatures, around 30ºC. This change, from an essentially athermic solvation energy to a highly exothermic one, in such a short range of temperatures, does not seem very physically realistic. However, it's clear that the $\Delta \bar{H}_s$ might be negative in both solvents with a mean value in the order of -10 kJ/mol to -12.5 kJ/mol, being difficult to conclude in which solvent the solvation enthalpy is more exothermic. The simulation results are practically 0 within the statistical error, which seems to indicate a need to increase the cross energy interaction between O_2 and both solvents. Once again it's difficult to decide which solvent needs the larger adjustment to its cross interaction parameter considering the statistical error and how large should those adjustments be considering the experimental data available. For CO_2 no adjustment was considered as there is no experimental ΔH_s to guide it and as mentioned previously the calculated solubilities seem to agree with the experimental results available.

Solutions of CO_2 and O_2 in (Hydrogenated+Perfluorinated) Mixtures

To get insight on the location of CO_2 and O_2 in mixtures of PFH+Hex and UFH+HexOH RDF analyses of these systems were performed. The nomenclature used to identify the carbon atoms is displayed in figures 10 and 11 for the PFH and UFH molecules, their hydrogenated counterparts have the same carbon numbers. The fluorinated carbons are referred as 'CFi' to distinguish them from the hydrogenated carbons, identified as 'Ci'.
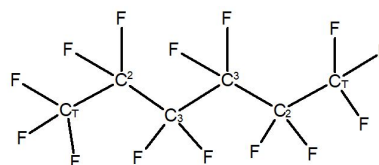

Figure 10: Molecular formula of Perfluorohexane with the nomenclature used to identify the carbon atoms.
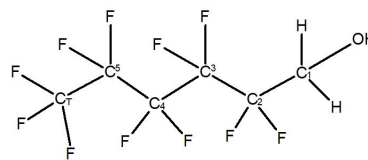

Figure 11: Molecular formula of Perfluorohexanol with the nomenclature used to identify the carbon atoms.

CO_2 in Pure Solvents For solutions of pure solvents containing one CO_2 molecule (infinite dilution) at 298.15K the RDFs were computed and are displayed in figures 12 and 13. For these RDFs the analyses were performed between the carbon of the carbon dioxide molecule and the carbons of the hydrogenated and fluorinated chains. In the case of UFH and HexOH, the RDFs between the carbon of CO_2 and the oxygen of the hydroxyl group were also included.
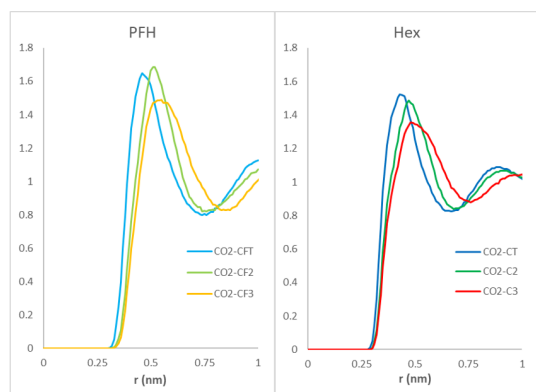
Figure 12: RDFs between the carbon of the CO_2 molecule and the carbons of PFH (left) and the carbons of Hexane (right) at 298.15K.
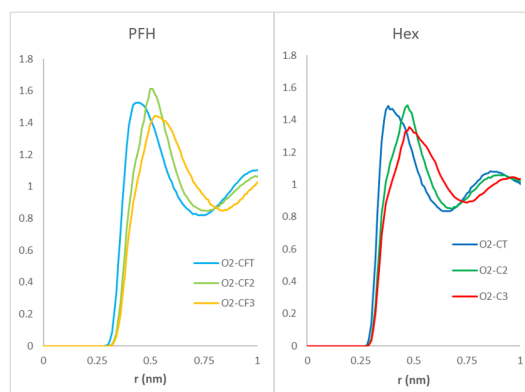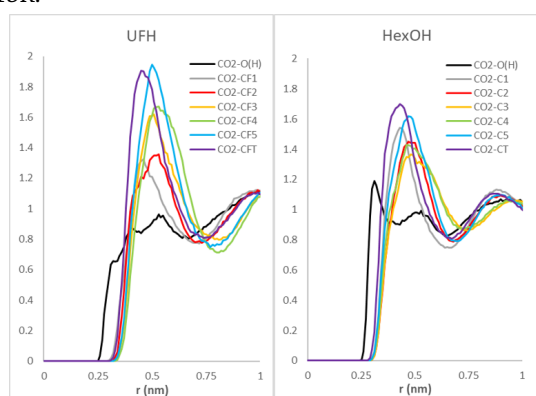

Figure 13: RDFs between the carbon of the CO_2 molecule and the carbons and oxygen of UFH (left), and the carbons and oxygen of hexanol (right) at 298.15K.

Figure 14: RDFs between O_2 and the carbons of PFH (left) and the carbons of hexane (right) at 298.15K.

Figure 15: RDFs between O_2 and the carbons and oxygen of UFH (left), and the carbons and oxygen of hexanol (right) at 298.15K.

As can be seen, for the PFH solution the most intense peak is the CO_2-CF2 interaction, then the terminal carbons and the lowest peak is the CO_2-CF3. For hexane the most intense peak is the CO_2-CT with the peaks decreasing along the chain. This seems to demonstrate a preference of the CO_2 molecule to neighbour the methyl group in the hydrogenated chain, this effect seems to be more preponderant in hexane than in PFH. In UFH the CO_2 molecule shows a clear preference for the end of the fluorinated chain. The most intense peaks are the CO_2-CFT and the CO_2-CF5. The intensity of the peaks decreases with the proximity to the OH group. The behaviour of the CO_2 molecule in hexanol is different as the highest peak is CO_2-CT followed by CO_2-C5, however the peaks don't decrease along the chain as it happened for the hexane. The third highest peak is the CO_2-C1, showing that CO_2 has a preference to be located at the end of the chain, tendentially near the terminal group or near the carbon bonded with the oxygen. The CO_2 atom is partially charged so it's possible that its interaction is relatively strong with the polar part of the hexanol molecule, the hydroxyl group, as can be seen by the peak demonstrated by the RDF CO_2-O(H). This way an inversion of the preferred carbons of the CO_2 molecule could occur, justifying the symmetric behaviour demonstrated.

O_2 in Pure Solvents The same procedure was done for O_2 in PFH, Hex, UFH and HexOH (infinite dilution) at 298.15K and the RDFs obtained are presented in figures 14 and 15.

Analysing the RDFs in figure 14, it's noticeable that in PFH the most intense peak corresponds to the O_2-CF2 interaction and the lowest peak is the O_2-CF3. For the Hex the most intense peak is the O_2-CFT with the intensity decreasing along the chain. The oxygen molecule seems to show a preference to neighbouring the methyl groups of the hydrogenated chains and in the fluorinated chains
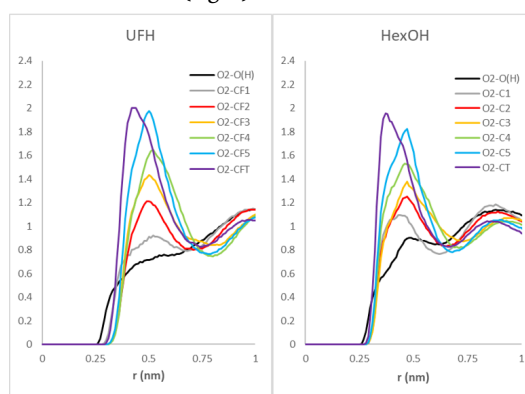
it appears to shows a preference for the CF2 carbons instead of the terminal carbons. These results are very similar to the ones obtained for the CO_2 molecule, so the conclusions taken are the same. In figure 15 it's possible to observe that the highest peak corresponds to that of the terminal group in both UFH and Hexanol (O_2-CFT and O_2-CT), a behaviour analogue to that of the CO_2 molecule in the same solvents. The peaks then decrease along the chain with the smallest peak being that of the hydroxyl group of the chain. It is also worth mentioning that the peak of the RDFs O_2-O(H) are both bellow one, meaning that the probability of the O_2 and the hydroxyl group being neighbours is very low in both alcohols. This is an indication that the O_2 molecule is preferentially located near the terminal group.

Local Compositions After analysing the RDFs of the mixtures, the local compositions of the alkane and alcohol mixtures around the solute molecules were calculated. In figures 16 and 17, the difference between the bulk and the local compositions of fluorine for the alkane and alcohol mixtures are shown, respectively.

From these figures it's possible to compare the concentration of fluorine around CO_2 or O_2 to the bulk concentration of the mixtures. It's noticeable that the local enrichment follows a similar pattern for CO_2 and O_2. For the alkane mixtures the results show a tendency to be negative which means that the concentration in fluorine near the solute molecules is smaller than the bulk concentration of fluorine, consequently, the hydrogen local concentration is higher than the hydrogen bulk concentration. This leads us to believe that CO_2 and O_2 appear to show a tendency to be near the hydrogenated solvent. For the alcohol mixtures we can see a preference of the solute molecules for the hydrogenated solvent in mixtures of 50% and 75% UFH and a preference for the fluorinated solvent in the mixture of 25%. When compar-
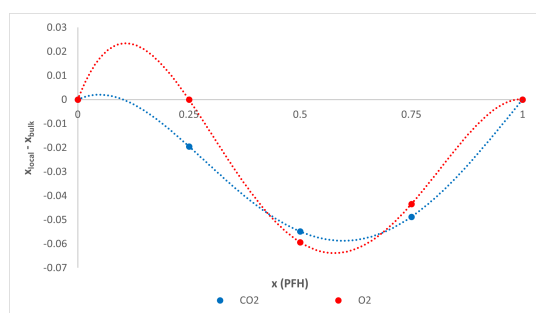
Figure 16: Local Enrichment of CO_2 (blue) and O_2 (red) as a function of bulk molar fraction of PFH in mixtures of PFH and Hexane at 298.15K
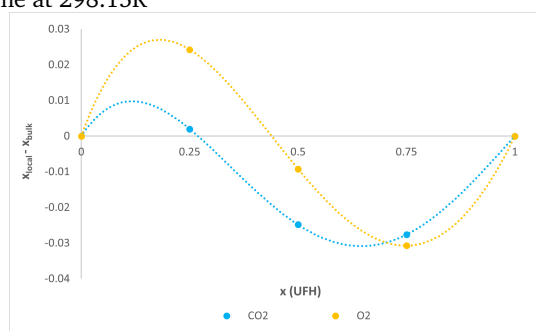

Figure 17: Local Enrichment of CO_2 (blue) and O_2 (yellow) as a function of bulk molar fraction of UFH in mixtures of UFH and Hexanol at 298.15K

ing both mixtures, the fluorine local enrichment in PFH+Hex is higher than in UFH+HexOH. This might result from the higher degree of nano-segregation in the alkane mixture that makes the difference in local composition more evident as the solvents are more segregated. It's important to emphasize that CO_2 and O_2 are said to be fluorophilic however from the present results that is not observed as they seem to exhibit a preference for the hydrogenated solvents.

Dynamics and Interaction Energies of Molecular Probes

Probe Dynamics and Interaction Energies in Perfluorohexane and Hexane The diffusion coefficients and hydrodynamic radius of CO_2 and O_2 in the alkane mixtures at 298.15K were calculated and are respectively displayed in figures 18 and 19.
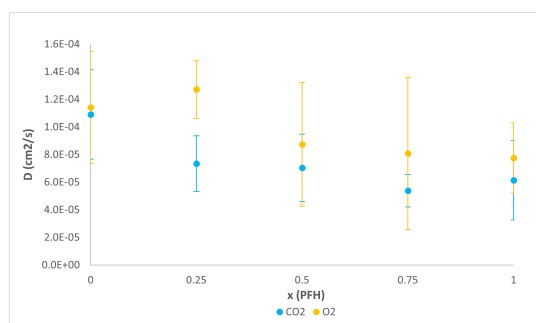

Figure 18: Diffusion Coefficient of CO_2 and O_2 in mixtures of PFH and Hexane at different compositions at 298.15K

Observing the diffusion coefficients in the alkane mixtures, figure 18, it's noticeable that the CO_2 molecule has a lower diffusion coefficient than O_2, so it's more difficult for CO_2 to move through the mixture. Another thing that is possible to conclude is that the diffusivity overall decreases with the increase in fluorinated compound, possibly as a consequence of the increase
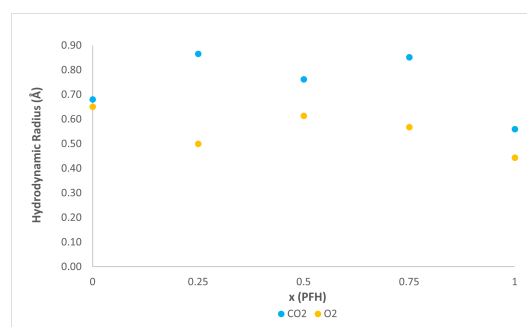

Figure 19: Hydrodynamic Radius of CO_2 and O_2 in mixtures of PFH and Hexane at different compositions at 298.15K

in the viscosity of the mixture. The only exception is the diffusivity of O_2 for a composition of 25% in PFH but it fits within the standard deviation. The hydrodynamic radius of O_2 is lower than that of CO_2, agreeing with the conclusions from the analysis of the diffusion coefficients. The overall conclusion seems to be that in the mixtures the motion of CO_2 is more difficult than in the pure solvents and for O_2 its movements get easier with the increase in PFH concentration. Since there is only one probe molecule in each system the results obtained have high statistical uncertainty associated, although the order of magnitude of the diffusion coefficients is correct. To get more exact results another method of calculation should be used or simulations of bigger systems with more solute and solvent molecules should be done to get better statistics in the MSDs, while maintaining the infinite dilution situation, resulting in a lower uncertainty associated. Once again, there are no experimental data to compare with the simulation results obtained. However, as previously mentioned, it is known that the experimental viscosities of these mixtures display large negative deviations. The present results are thus difficult to interpret.

The interaction energies between CO2/O2 and the alkane solvents were determined and the results are displayed in figures 20 and 21.
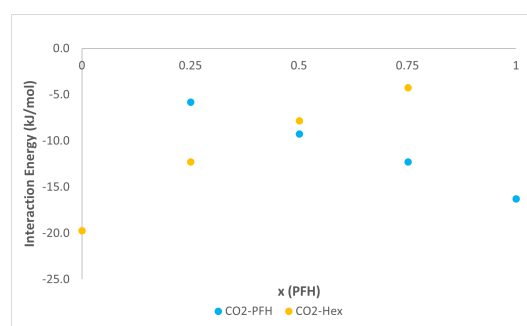

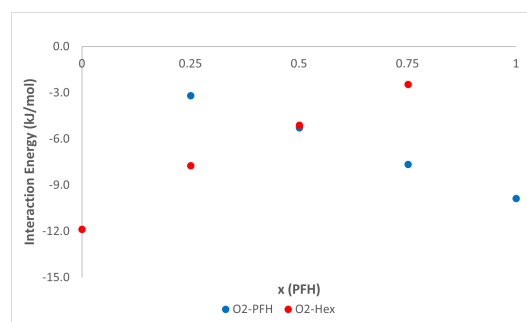**Figure 20:** Interaction Energy of CO_2 with PFH and Hexane at 298.15K

Figure 21: Interaction Energy of O_2 with PFH and Hexane at 298.15K

Examining the results obtained it's possible to note that in the pure solvents the IE is larger (more negative) between the probes and hexane, and CO_2 interacts more strongly with both solvents than O_2. This is in agreement with the results obtained for the hydrodynamic radius and diffusivities, since CO_2 interacts more strongly with the solvents it means it's more difficult for CO_2 to move through the liquid mixtures, so the diffusion coefficients are lower. Comparing the interaction energy of each probe with both pure solvents, it's possible to see that CO_2 and O_2 have a stronger interaction with Hex than with PFH, even though their diffusivity is higher in hexane. This is probably due to the contribution of viscosity in the diffusion coefficients, as the viscosity of PFH is higher than the viscosity of Hex it results in an enhanced movement of CO_2 and O_2 in hexane. As expected, the IE of both solutes vary linearly with the solvents concentration. However, a slight deviation to lower IE (less negative) can be observed for both O_2 and CO_2 with hexane, particularly at low concentration of the fluorinated component. This result is compatible with the results obtained for the local concentration of each solute.

Probe Dynamics and Interaction Energies in Perfluorohexanol and Hexanol

The diffusion coefficients and hydrodynamic radius of CO_2 and O_2 in the alcohol mixtures were also determined, and the results are presented in figures 22 and 23, respectively.
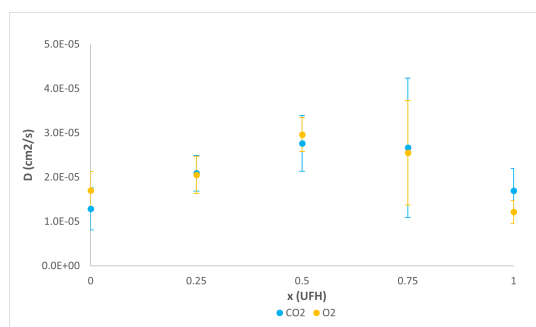

Figure 22: Diffusion Coefficient of CO_2 and O_2 in mixtures of UFH and Hexanol at different compositions at 298.15K
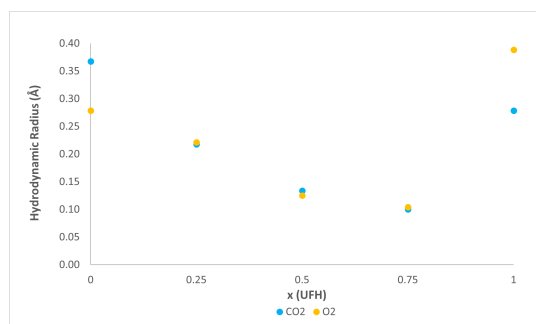

Figure 23: Hydrodynamic Radius of CO_2 and O_2 in mixtures of UFH and Hexanol at different compositions at 298.15K

For the UFH+HexOH mixtures it's visible that the diffusion coefficients of CO_2 and O_2 are lower than in the alkane mixtures probably due to the formation of a hydrogen bond network between the hydroxyl groups making movement more difficult for the probe molecules. Interestingly, in this case the diffusion coefficients don't decrease with the increase in UFH concentration but instead the mixtures show a positive deviation, resulting in higher diffusion coefficients than in pure solvents. In agreement, the hydrodynamic radius show a negative deviation, showing that the mobility of the probe molecules is higher in the mixtures than in pure solvents. This can be a good indication that the hydrogen bond network in the alcohol mixtures is less effective than in the

pure alcohols, making the motion of the solutes easier throughout the mixtures than throughout the pure solvents.

The interaction energies between CO_2/O_2 and the alcohol solvents were also determined and the results are displayed in figures 24 and 25.
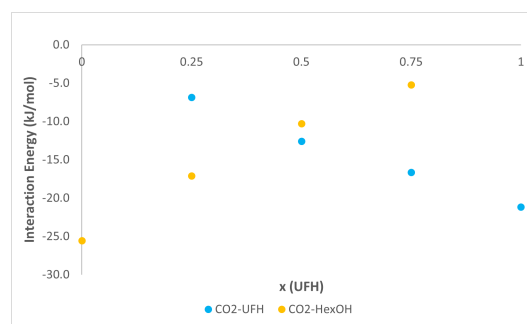

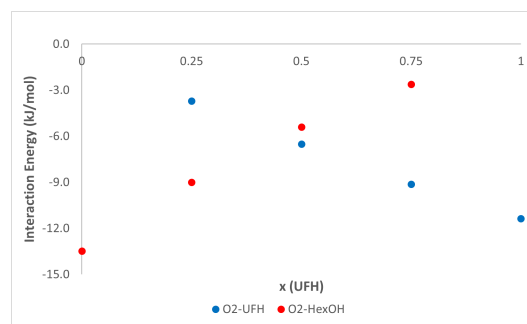**Figure 24:** Interaction Energy of CO_2 with UFH and Hexanol at 298.15K

Figure 25: Interaction Energy of O_2 with UFH and Hexanol at 298.15K

The interaction energy between CO_2 and the alcohol solvents is larger (more negative) than the IE of O_2, just like in the alkane mixtures. But the interactions with the alcohol solvents are stronger than with the alkane solvents. A possible explanation is the existence of the hydroxyl group (polar component of the solvent molecules) in the alcohols strengthening the interactions with the probe molecules. When comparing these results with the hydrodynamic radius and the diffusivity of the solute molecules, it's noticeable that CO_2 interacts more strongly with HexOH than O_2, which is reflected in the hydrodynamic radius as it is lower for O_2, meaning it moves more easily through the liquid. However, in UFH the hydrodynamic radius is higher for O_2 even though the interaction between O_2 and UFH is weaker than the interaction of CO_2 and UFH. As in the case of Hex+PFH, the IE of both solutes vary linearly with the solvents concentration. Again, a slight deviation to lower IE (less negative) can be observed for both O_2 and CO_2 with hexane, particularly at low concentration of the fluorinated component. These deviations are compatible with the results obtained for the local concentration of the solutes, although in the case of the alcohols, the differences between local concentration and nominal concentration are smaller.

Conclusions and Future Work

The objectives of this work were to assess and compare the affinity of respiratory gases, in particular CO_2 and O_2, often said to be fluorophilic, towards hydrogenated and fluorinated solvents using molecular dynamics simulations as a tool. Information about the dynamics of O_2 and CO_2 solutions was also sought.

Additionally, mixtures of hydrogenated and perfluorinated fluids are known to form nano-segregated hydrogenated and perfluorinated domains, that xenon atoms are able to detect dissolving

preferentially in hydrogenated environments. Following the same strategy, the ability of CO_2 and O_2 as test particles, to detect hydrogenated and perfluorinated nano-domains in mixtures of hydrogenated and fluorinated liquids, was intended, an effect that has not yet been experimentally or theoretically detected.

With these objectives in mind, a number of important conclusions could be reached.

The density and excess molar volume of the simulated mixtures of hydrogenated and perfluorinated solvents show a good agreement with experimental data. This validates the force field used to study the behavior of these mixtures. Moreover, analyses of the radial distribution functions between fluorine and hydrogen confirm the existence of nano-segregation between the hydrogenated and perfluorinated chains resulting in the formation of fluorinated and hydrogenated domains. This segregation is more evident in the mixtures of Hex+PFH, probably due to the existence of a network of H-bonds in the alcohol mixtures that decrease the effect of unfavorable dispersion forces present from the apolar part of the chains.

The Henry's constants and the solvation enthalpies of the solutes in pure hexane and PFH also reproduce well the existing experimental data, contributing to the validation of the simulations performed and more importantly validating the model used to describe the interactions between the solutes and the solvents. Moreover, the simulation results confirm that the solubility of CO_2 and O_2 in perfluorinated solvents is almost two times larger than in hydrogenated solvents.

The RDFs show that in the pure solvents, CO_2 seems to demonstrate a preference to neighbor the terminal groups of the solvents. In Hex+PFH mixtures it seems to prefer the proximity of hydrogenated groups, as CO_2 is locally enriched in hydrogen. In the UFH+HexOH mixtures, however, CO_2 seems to prefer domains enriched in hydrogenated groups for mixtures containing 50% - 75% of UFH, while for mixtures of low UFH concentration CO_2 shows a preference for fluorinated domains. The behavior of O_2 is similar to that of CO_2 in pure solvents, exhibiting a preference for the terminal groups of the solvents. In mixtures of Hex+PFH, O_2 also seems to prefer the hydrogenated domains. For the alcohol mixtures, it also seems to prefer hydrogenated domains for compositions of 75% and 50% in UFH, and fluorinated domains for mixtures with 25% of UFH.

Thus, in general, the simulation results do not indicate any preferential location of O_2 and CO_2 towards perfluorinated solvents. On the contrary, both gases seem to dissolve preferentially within hydrogenated environments, except in a narrow range of concentration, at low fluorinated content. This result is the opposite of what could be expected since these probes are said to be fluorophilic. Xenon, a particle that is known to be fluorophobic, is able to distinguish between hydrogenated and fluorinated domains and preferentially dissolve within the hydrogenated. Apparently, O_2 and CO_2 in spite of their enhanced solubility in fluorinated solvents, when both types of chains are present also "prefer" hydrogenated domains. These results are in line with the interaction energies obtained in the simulations. The enhanced solubility of the gases in the fluorinated solvents is thus probably due to the existence of cavities intrinsic to the liquid structure of the perfluorinated solvents.

Regarding the dynamics of the O_2 and CO_2 solutions, the simulated diffusion coefficients in mixtures of Hex+PFH, as could be expected, CO_2 (larger particle) has a lower diffusion coefficient than O_2, and both decrease with the increase in PFH concentration, a consequence of the increasing viscosity of the mixtures. The estimated hydrodynamic radius of the probes seems to slightly decrease with the increase in PFH concentration. The interaction energy between CO_2 and the solvents is larger (more negative)

than that of O_2, and both probes interact more strongly with hexane. As for the UFH+HexOH mixtures, the diffusion coefficients of the probe molecules display positive deviation when compared to the pure solvents. The hydrodynamic radius exhibits a negative deviation being lower in the mixtures and higher in pure solvents. This indicates that they move more quickly through the mixtures. Both probes interact more strongly with the hydrogenated compounds. These results can be a good indication that the hydrogen bond network in the alcohol mixtures is less effective than in the pure alcohols, making the motion of the solutes easier through the mixtures than through the pure solvents. A comment that should be made is the fact that the diffusion results have a much higher uncertainty as the statistics resulting from only one probe molecule are not very good. There is also no experimental data available to compare and assess their validity.

The validation of the simulation results was in many cases very difficult due to lack of experimental data. In other cases, the large statistical uncertainty inherent to some simulation methods also prevented reaching some of the desired conclusions. In some cases, more and longer simulation runs would be important, but were unfeasible during the available time.

The present results introduce new interesting questions that could be carried out as a follow up of this study. More in depth studies on the properties of these mixtures could be done, in particular obtaining experimental data on the diffusion coefficients. Longer simulations to obtain results with less uncertainty and at different temperatures would also be important. The experimental determination of the solubility of CO_2 in perfluorinated compounds, namely in perfluorohexane, would be very important, as there is a lack of experimental data on these solutions. Also important and interesting, would be the experimental determination of the solubility of CO_2 and O_2 in mixtures of hydrogenated and perfluorinated solvents. Equivalent studies should be carried out for different mixtures, or with other important molecules like water, xenon or nitrogen.

References

[1] Morgado, P., J. Black, J.B. Lewis, C.R. Iacovella, C. McCabe, L.F.G. Martins, and E.J.M. Filipe. *Fluid Phase Equilibria*, pages 161–165, 11, ISSN 03783812.

[2] Morgado, P., C.M.C. Laginhas, J.B. Lewis, C. McCabe, L.F.G. Martins, and E.J.M. Filipe. *Journal of Physical Chemistry B*, pages 9130–9139, July, ISSN 15205207.

[3] Morgado, P., J.B. Lewis, C.M.C. Laginhas, L.F.G. Martins, C. McCabe, F.J. Blas, and E.J.M. Filipe. *Journal of Physical Chemistry B*, pages 15013–15023, 12, ISSN 15205207.

[4] Morgado, P., L.F.G. Martins, and E.J.M. Filipe. *Physical Chemistry Chemical Physics*, pages 3742–3751, ISSN 14639076.

[5] Morgado, P., A.R. Garcia, L.M. Ilharco, J. Marcos, M. Anastácio, L.F.G. Martins, and E.J.M. Filipe. *Journal of Physical Chemistry B*, pages 10091–10105, 9, ISSN 15205207.

[6] Duarte, P., M. Silva, D. Rodrigues, P. Morgado, L.F.G. Martins, and E.J.M. Filipe. *Journal of Physical Chemistry B*, pages 9709–9717, 8, ISSN 15206106.

[7] Ebnesajjad, S.: *Concise handbook of fluorocarbon gases*, 2021.

[8] Freire, M.G., P.J. Carvalho, A.J. Queimada, I.M. Marrucho, and J.A.P. Coutinho. *Journal of Chemical and Engineering Data*, pages 1820–1824, 9, ISSN 00219568.

[9] Silva, G.M.C., J. Justino, P. Morgado, M. Teixeira, L.M.C. Pereira, L.F. Vega, and E.J.M. Filipe. *Journal of Molecular Liquids*, 2, ISSN 01677322.

[10] Aryal, M., C.D. Arvanitis, P.M. Alexander, and N. McDannold. *Advanced Drug Delivery Reviews*, pages 94–109, 6, ISSN 18728294.

[11] Kwan, J.J., M. Kaya, M.A. Borden, and P.A. Dayton. *Theranostics*, pages 1174–1184, ISSN 18387640.

[12] Wesseler, E.P., R. Iltis, and L.C. Clark. *Journal of Fluorine Chemistry*, pages 137–146.

[13] Evans, F.D. and R. Battino. *J. Chem. Thermodynamics*, pages 753–760.

[14] Raveendran, P. and S.L. Wallen. *Journal of Physical Chemistry B*, pages 1473–1477, 2, ISSN 10895647.

[15] Cece, A., S.H. Jureller, J.L. Kerschner, and K.F. Moschner: *Molecular modeling approach for contrasting the interaction of ethane and hexafluoroethane with carbon dioxide*, 1996.

[16] Dardin, A., J.M. Desimone, and E.T. Samulski: *Fluorocarbons dissolved in supercritical carbon dioxide. nmr evidence for specific solute-solvent interactions*, 1997.

[17] Yee, G.G., J.L. Fulton, and R.D. Smith. *The Journal of Physical Chemistry*, pages 6172–6181.

[18] Yonker, C.R. *Journal of Physical Chemistry A*, pages 685–691, 2, ISSN 10895639.

[19] Gomes, M.F.C. and A.A.H. Pádua. *Journal of Physical Chemistry B*, pages 14020–14024, 12, ISSN 15206106.

[20] Monteiro, R.M.G.: *Nano-organization of fluorinated amphiphiles*, 2020.

[21] Abraham, M., B. Hess, D.V.D Spoel, and E. Lindahl: *Gromacs reference manual version 2018*, 2018.

[22] Parrinello, M. and A. Rahman. *Journal of Applied Physics*, pages 7182–7190, ISSN 00218979.

[23] Nosé, S. *Molecular Physics*, pages 255–268, ISSN 13623028.

[24] Maxwell, D.S., J. Tirado-Rives, and W.L. Jorgensen. *Article in Journal of the American Chemical Society*, page 99.

[25] Watkins, E.K. and W.L. Jorgensen. *Journal of Physical Chemistry A*, pages 4118–4125, 4, ISSN 10895639.

[26] Siu, S.W.I., K. Pluhackova, and R.A. Böckmann. *Journal of Chemical Theory and Computation*, pages 1459–1470, 4, ISSN 15499618.

[27] Pluhackova, K., H. Morhenn, L. Lautner, W. Lohstroh, K.S. Nemkovski, T. Unruh, and R.A. Böckmann. *Journal of Physical Chemistry B*, pages 15287–15299, 12, ISSN 15205207.

[28] Chitra, R. and P.E. Smith. *Journal of Chemical Physics*, pages 5521–5530, 9, ISSN 00219606.

[29] Pádua, A.A.H. *Journal of Physical Chemistry A*, pages 10116–10123, 10, ISSN 10895639.

[30] Harris, J.G. and K.H. Yung. *J. Phys. Chem*, pages 12021–12024.

[31] Miyano, Y. *Fluid Phase Equilibria*, pages 1999–2028.

[32] Bohn, M., S. Lago, J. Fischer, and F. Kohler. *Fluid Phase Equilibria*, pages 137–151.

[33] Song, W., P.J. Rossky, and M. Maroncelli. *Journal of Chemical Physics*, pages 9145–9162, 11, ISSN 00219606.

[34] Silva, G.M.C., P. Morgado, P.Lourenço, M. Goldmann, and E.J.M. Filipe. *Proceedings of the National Academy of Sciences of the United States of America*, pages 14868–14873, 7, ISSN 10916490.

[35] Hess, B., H. Bekker, H.J.C Berendsen, and J.G.E.M Fraaije: *3 lincs: a linear constraint solver for molecular simulations*, 1997.

[36] Widom, B. *The Journal of Chemical Physics*, pages 2808–2812, ISSN 00219606.

[37] Jamali, S.H., A. Bardow, T.J.H. Vlugt, and O.A. Moultos: *A generalized form for finite-size corrections in mutual diffusion coefficients of multicomponent mixtures obtained from equilibrium molecular dynamics simulation*, 2020.

[38] *Boltzmann constant.* https://www.nist.gov/si-redefinition/kelvin-boltzmann-constant.

[39] M.A.P.Costa: *Property data and phase equilibria for the design of chemical processes involving carbon dioxide*, 2017.

[40] Lepori, L., E. Matteoli, A. Spanedda, C.Duce, and M.R. Tiné. *Fluid Phase Equilibria*, pages 119–134.

[41] Afonso, J.O.M.: *Transport properties of fluorinated surfactants: viscosity and diffusion of mixtures involving fluorinated alcohols*, 2018.

[42] Pollack, G.L. and J.F. Himm. *The Journal of Chemical Physics*, pages 3221–3229, ISSN 00219606.

[43] Kennan, R.P. and G.L. Pollack. *The Journal of Chemical Physics*, pages 517–521, ISSN 00219606.

[44] Bonifácio, R.P., E.J.M. Filipe, C. McCabe, M.F.C. Gomes, and A.A.H. Pádua. *Molecular Physics*, pages 2547–2553, 8, ISSN 00268976.

[45] Dias, A. M.A., R. P. Bonifácio, I. M. Marrucho, A. A.H. Pádua, and M. F. Costa Gomes. *Physical Chemistry Chemical Physics*, pages 543–549, ISSN 14639076.

[46] Bonifácio, R.P.M.F., L.F.G. Martins, C. McCabe, and E.J.M. Filipe. *Journal of Physical Chemistry B*, pages 15897–15904, 12, ISSN 15205207.